CHALMERS
UNIVERSITY OF TECHNOLOGY

Integrated-EBG Ridge Waveguide and Its Application to an E-Band Waveguide 32×32 Slot Array Antenna

Citation for the original published paper (version of record):
He, Z., Jin, C., An, S. et al (2020). Integrated-EBG Ridge Waveguide and Its Application to an E-Band Waveguide 32×32 Slot Array
Antenna. IEEE Open Journal of Antennas and Propagation, 1: 456-463.
http://dx.doi.org/10.1109/OJAP.2020.3017887

(article starts on next page)

IEEE Open Journal of
Antennas and Propagation

Received 3 July 2020; revised 4 August 2020; accepted 10 August 2020. Date of publication 26 August 2020; date of current version 8 September 2020.

Digital Object Identifier 10.1109/OJAP.2020.3017887

Integrated-EBG Ridge Waveguide and Its Application to an E-Band Waveguide 32×32 Slot Array Antenna

ZHONGXIA SIMON HE [1,2] (Senior Member, IEEE), CHENG JIN [3] (Senior Member, IEEE), SINING AN [2], LINGWEN KONG [3], AND JINLIN LIU [4] (Member, IEEE)

[1]Research and Development Department, SenWellen (Shenzhen) Communications Technologies Company Ltd., Shenzhen, China

[2]Mirowave Electronics Laboratory, Department of Microtechnology and Nanoscience (MC2), Chalmers University of Technology, 412 96 Gothenburg, Sweden

[3]School of Information and Electronics, Beijing Institute of Technology, Beijing 100081, China

[4]State Key Laboratory of Millimeter Waves, Southeast University, Nanjing 210096, China

CORRESPONDING AUTHOR: S. AN (e-mail: sininga@chalmers.se)

This work was supported in part by the National Key Research and Development Program of China under Grant 2019YFB1803200, in part by the National Natural Science Foundation of China (NSFC) under Grant 61871036, and in part by the Open Project of the State Key Laboratory of Millimeter Waves under Grant K202018.

ABSTRACT A methodology of designing an E-band waveguide 32 × 32 slot array antenna with high-efficiency and low-cost manufacturing characteristics is proposed in this article, which is based on an integrated electronic bandgap (EBG) ridge waveguide designed by integrating a cross rectangle-hollow EBG structures in the conventional ridge waveguide. The integrated EBG structure intercepts the leakage from the unconnected gap in between the two metallic plates of the waveguide, and then it decreases the manufacturing cost without using the diffusion bonding technology and multi-layer welding assembly process. The design guideline is discussed, and then the antenna is fabricated. The measured radiation characteristics are in good agreement with predicted ones, which confirms that the proposed cross rectangle-hollow EBG structures is an attractive candidate of high-performance millimeter wave antenna.

INDEX TERMS Antenna array, E-band antenna, electromagnetic gap, low-cost, ridge waveguide.

I. INTRODUCTION

COMMUNICATION systems in E-band covering 71-76 GHz and 81-86 GHz frequency bands have been a subject of significant importance recently, because they have relatively small atmospheric path loss compared with nearby frequency bands and the wireless systems have the potential to become a cost-effective choice to the optic fiber systems [1]–[3]. The development of E-band high-gain antennas has witnessed explosive growth driven by outdoor point-to-point backhaul applications [4]. Reflector antennas are the traditional way to realize the high-gain antennas, but they usually suffer from the weakness of large geometric structures.

Another attractive approach is using thin planar millimeter-wave (mmWave) antennas, which are with a lower profile and more suitable for the E-band point-to-point backhaul systems. Substrate integrated waveguide (SIW) is an attractive candidate to overcome the bulky structure by exploiting the features of rectangular waveguide. Several planar SIW antennas have been proposed with the advantages of low-cost, easy-to-fabricate based on PCB technique, and convenient to be connected to planar active components through coplanar waveguide [5]–[13]. However, SIWs usually suffer from increased dielectric losses as frequency increases [14]–[17].

A kind of thin planar slot array antennas has been achieved based on conventional waveguide technology [18], [19], and they are high efficiency without dielectric losses [20]. However, the required manufacturing tolerances for the multilayer welding assembly process become very strict

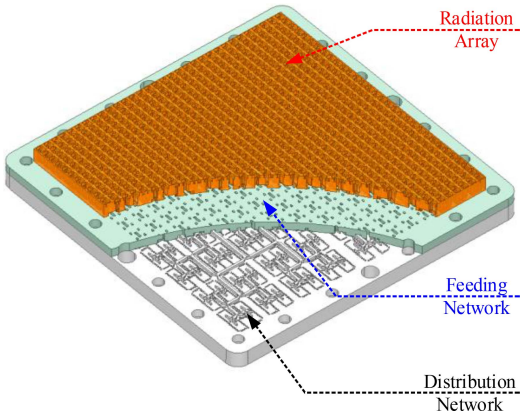

FIGURE 1. Breakdown drawing of the array antenna.

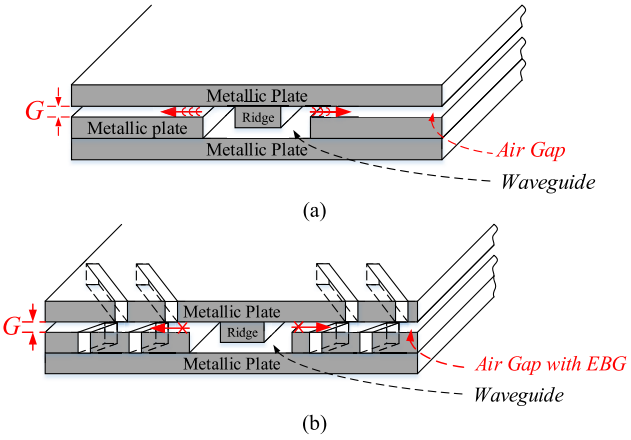

FIGURE 2. Configuration of the gapped ridge waveguides. (a) Normal ridge waveguide with small leakage gap between top and bottom layers. (b) Proposed gapped ridge waveguide with EBG structure realized by cross-shaped grooves. G = 0.005mm.

as the operating frequency increases. The issue of even a slightly discrepancy concerning the structure alignment may destroy the performance of antennas, which is particularly severe in the case of antennas operating at mmWave frequency bands, where the small tolerances will result in mismatching of feeding network, leakage loss and lower the gain of antennas, and even disable the antennas [18], [21]. A diffusion bonding technology is usually applied to implement the robust contact of the multi-layer of the waveguide antennas without leakage, but this manufacturing technology is generally expensive and not suitable for massive production. Without the possibility of low-cost techniques, wide-scale adoption has remained elusive for the high-efficiency waveguide antennas.

Hence, efficient and low-cost antennas become more and more significant with the rapid development of wireless communication systems [22]–[24]. Comparing with expensive high-precision fabrication techniques, it is better to utilize advanced design to counterbalance the rigorous manufacturing and assembly requirement, although it will increase the cost in design and simulation stages. Then, a new kind of gap-waveguides, such as inverted microstrip gap waveguide (IMGW), groove-ridge-inverted microstrip, microstrip-ridge gap waveguides (RGWs), and groove gap waveguide (GGW) have been proposed recently, and it provides novel low loss technologies that promising replaces the conventional waveguides [25]–[28].

In this article, a methodology of integrated-EBG ridge waveguide with high-efficiency and low-cost manufacturing characteristics is proposed as shown in Fig. 1, and an E-Band waveguide 32x32 slot array antenna is designed based on the studied structure. The integrated-EBG ridge waveguide is investigated, and it is found that the proposed structure can inevitably decrease the manufacturing cost without using the diffusion bonding technology and multi-layer welding assembly process. Also, it does not increase the design complexity for the waveguide slot array antennas, and a single-layered series feeding network is applied as usual, which is simple compared with the aforementioned corporate feeding networks.

II. INTEGRATED-EBG RIDGE WAVEGUIDE AND POWER DIVIDER DESIGN

The proposed waveguide slot array antenna is shown in Fig. 1, which includes radiation array, feeding network, and power divider distribution network. The antenna is excited through a standard E-band rectangular waveguide (WR-12) at the bottom. Each radiation unit cell consists of 2×2 radiation slots sub-array, and the sub-array is made up of the backed cavities where four neighbouring slots share a common feeding cavity to improve wideband response while contains the size of distribution networks [18], [25]–[27], [29].

A. CROSS RECTANGLE-HOLLOW EBG STRUCTURE

The feeding network of the antenna consists of two 16-way ridge waveguide power dividers, taking electromagnetic waves from a central transition power divider to the 2×2 radiating slot sub-array. The rectangular ridge waveguide is realized by combining two vertically stacked parts including the top metallic plate with ridge and the bottom metal plate with rectangle waveguide. It is assumed that an air-gap with thickness of G is between the two thin metallic plates if normal assembly technology is used without multi-layer welding or diffusion bonding technology as shown in Fig. 2(a). However, the leakage loss because of the small gap through the ridge waveguide is non-negligible for the mmWave frequency antenna. Hence, it is important to investigate an efficient and high-quality combination technology to counterbalance the rigorous manufacturing and assembly requirement.

An integrated electronic bandgap (EBG) ridge waveguide is proposed to intercepting the aforementioned leakage. In order to avoid increasing the design complexity for the power divider, the conventional ridge waveguide as shown in Fig. 2(a) are upgraded only by integrating the proposed cross rectangle-hollow EBG structures as shown in Fig. 2(b). The integrated-EBG rectangular ridge waveguide is achieved by assembling two vertically stacked parts, and the air-gap

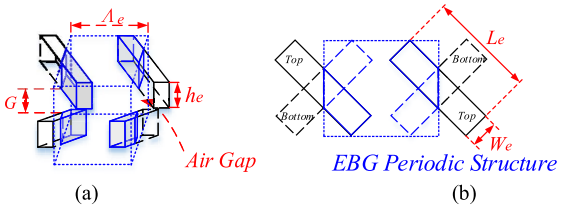

FIGURE 3. Configuration of the unit cell of the gapped cross-shaped groove EBG structure. (a) Perspective views. (b) Cross-sectional view. he = 0.2, We = 0.25, Le = 0.7, and Λe = 0.8 . All are in mm.

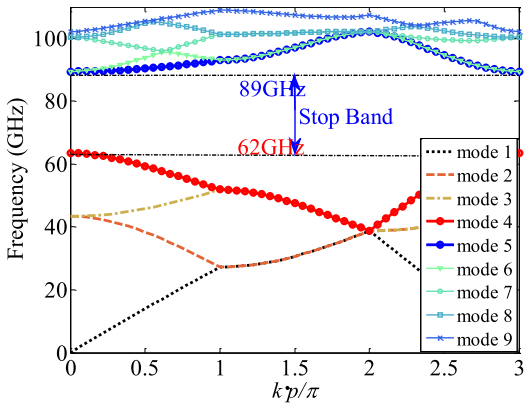

FIGURE 4. Dispersion diagram for the gapped cross-shaped groove EBG for the infinite periodic unit cell. Ae = 0.8mm, and G = 0.005mm.

with a thickness of G still exists in-between the two metallic plates. A periodic 45° rotated rectangular hollows with wide of W_e, length of l_e and height of l_e are excavated in the bottom layer of the ridge waveguide just near the original ridge waveguide, and another array of rectangular hollows with the same dimensions as the bottom hollows but rotated by −45° are cut in the top metallic plate layer as shown in Fig. 2(b). The period of the EBG unit cell is Λ_e. Then, an array of cross rectangle-hollow EBG structures with a small gap in between the two plates is integrated, as a detailed configuration is shown in Fig. 3.

Fig. 4 presents the dispersion diagram with the first 9 modes of the unit cells for the designed cross rectangle-hollow EBG structure with a $G = 0.005$um gap based on the full-wave analysis by using commercial ANSYS HFSS software. It can be seen that no mode is supported by the structure from 62 GHz to 89 GHz, therefore a desired stopband is obtained even though the structure consists of an unconnected gap in between the two metallic plates. Hence, the leakage in gaped ridge waveguide structures will be eliminated in this stopband range, and a high-performance low-loss waveguide with a gap in between top and bottom plates is obtained. Moreover, the structure can be manufactured just by using of low-cost assembly methods, such as metallic screws.

B. POWER DIVIDER DESIGN

Furthermore, the power divider realized by the integrated-EBG rectangular gap ridge waveguide is designed and investigated. The space between antenna radiation slots is usually very limited, so that a ridge waveguide is applied to provide a more compact configuration for the distribution feeding network.

TABLE 1. The parameters of the power divider with 2 × 2 subarray radiator.

Parameter	Value (mm)	Parameter	Value (mm)	Parameter	Value (mm)
L_{r1}	0.51	L_{r2}	0.44	L_{r3}	1.27
L_{r4}	2.57	L_{w1}	11.55	L_{w2}	3.02
R_{w1}	1.20	R_{w2}	0.80	R_{r3}	1.50
W_w	1.30	W_r	0.80	P_e	1.14
W_{r1}	0.96	W_{r2}	1.08	W_{r3}	2.86
h_{pD}	0.50	h_w	1.30	h_r	0.95
h_{FN}	3.30	φ_{w1}	0.90	A_r	1.23

Before designing the practical power divider with a gap in between top- and bottom-layers, a power divider with ideal rectangular ridge waveguide is designed first without the gap, and its configuration is similar to the one as shown in Fig. 5(a) and the dimensions are the same as shown in Fig. 5(b-e) but without the proposed integrated EBG-structures. The blue lines as shown in Fig. 6(a) illustrates the simulated scattering parameters of the ideal power divider, and it shows that good performance has been achieved. Then, an air-gap with a thickness of G is added between the two thin metallic plates as assumed in the actual assembly process, and the simulated scattering parameters are also shown in Fig. 6(b-e). The result shows the power divider fails to work with the air-gap due to leakage loss.

Afterward, the studied cross rectangle-hollow EBG structure is integrated as shown in Fig. 5, and its detailed dimensions is shown in Fig. 5(b-e). The periodic EBG texture providing a stopband for the desired frequency band will eliminate unwanted leakages. Acceptable performance is obtained even with air gaps, as demonstrated in Fig. 6(a). Because the two thin metallic plates of the power divider are allowed not to be physical contacted, and no strong field leakage occurs between the layers, it leads an obvious mechanical assembly flexibility.

In addition, an one to four power divider is also designed, and the simulated results are also given as shown in Fig. 6(c). The reflection coefficients are less than −15 dB, and the magnitude imbalances are ±0.1 dB in the working frequency band. Another T-junction power divider through a WR-12 rectangular waveguide port locates at the bottom of the whole structure to the proposed gap ridge waveguide with cross rectangle-hollow EBG structure is used in our feeding network as the inset figure shown in Fig. 7. The T-junction then has been optimized for the minimum reflection coefficient, and the corresponding S-parameters are shown in Fig. 7, in which the excellent power distribution is obtained.

III. WAVEGUIDE SLOT ARRAY ANTENNA DESIGN

A. DESIGN OF 2 × 2 SUBARRAY RADIATOR

The ridge waveguide slot array antenna presented in this article vertically consists of three waveguide layers, as shown in Fig. 1, i.e, the radiation array, the feeding network, and the power divider distribution network. The gap ridge waveguide with cross rectangle-hollow EBG structure contributes easily mechanical assembly power divider design by using

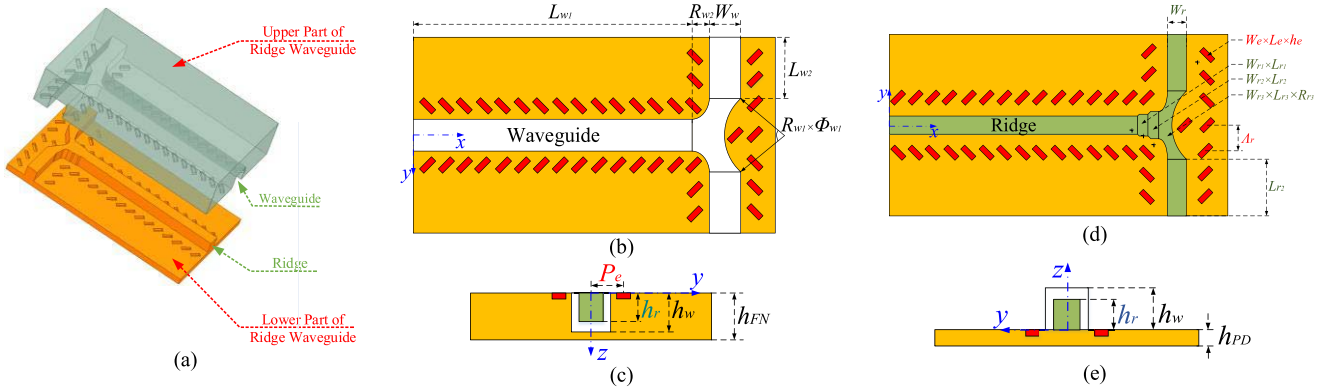

FIGURE 5. Configuration of the power divider realized by the gapped ridge waveguide with cross-shaped groove EBG structure. (a) Perspective view. (b) Top view and (c) Side view of the waveguide layer. (d) Top view and (e) Side view of the ridge layer. The parameters of the power divider are provided in Table 1.

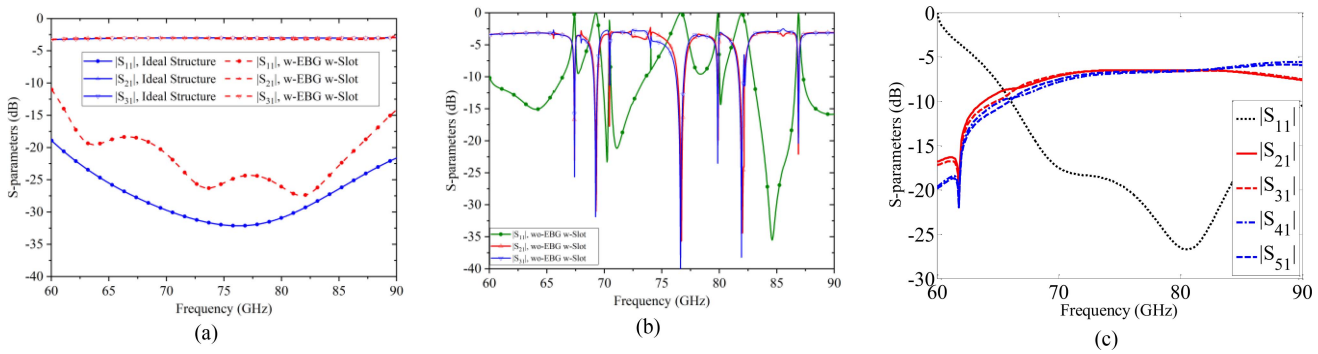

FIGURE 6. Simulated S-parameters of the power dividers. (a) S-parameters for the power divider realized by the ideal ridge waveguide without the gap between two layers, and for the power divider realized by the proposed gapped ridge waveguide with cross-shaped groove EBG structure. (b) S-parameters for the power divider realized by the gapped ridge waveguide but without the cross-shaped groove EBG structure. (c) S-parameters for the 1-to-4 power divider realized by the proposed gapped ridge waveguide with cross-shaped groove EBG structure.

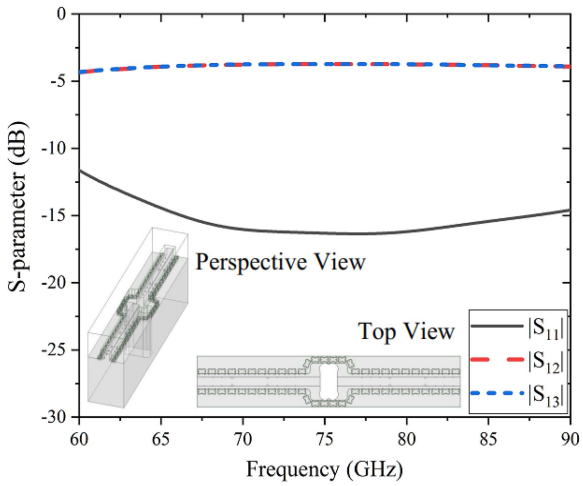

FIGURE 7. Configuration and simulated scattering parameters of the power dividers with a waveguide to ridge waveguide transition.

a parallel-plate stopband over a specific frequency range covering from 62 GHz to 89 GHz as shown in Fig. 4 and 6(a).

Then, small space will be left for the waveguide radiator after arranging the distribution feeding network, and the 32 × 32 ridge waveguide slot array antenna is divided by 22 subarray radiator in order to enlarge the physical size of the element spacing. It should be pointed out that the width of all the gap and metallic plates are designed above 0.3 mm herein. The configuration of 2 × 2 subarray radiator of the designed antenna is illustrated in Fig. 8, which is constituted by three waveguide layers of the feeding layer, cavity layer and radiating layer with dimensions shown in Table 2.

The studied gap ridge waveguide power dividers are combined and modeled to build the entire distribution network, as illustrated in Fig. 1, and then the distribution network feeds all slots with the same amplitude and the phase through a vertical metal-septum waveguide feeding structure. As shown in Fig. 8, the feeding layer transition from gap ridge waveguide to a rectangular coupling slot is in the bottom of the 2 × 2 subarray radiator.

The electromagnetic wave is then transmitted to the middle cavity layer through the rectangular coupling slot, which consists of backed cavities with symmetrical metallic blocks and four rectangular metallic bricks inside the cavities as shown in Fig. 8. The cavity layer distribution network can be seen by combining one folded 1-to-2 H-T waveguide power divider with two vertical 1-to-2 E-T waveguide power dividers, and the cavity layer introduces a 1-to-4 distribution network with the advantage of supplying more space for the bottom distribution power divider network. It should be noticed that the symmetrical metallic blocks will suppress

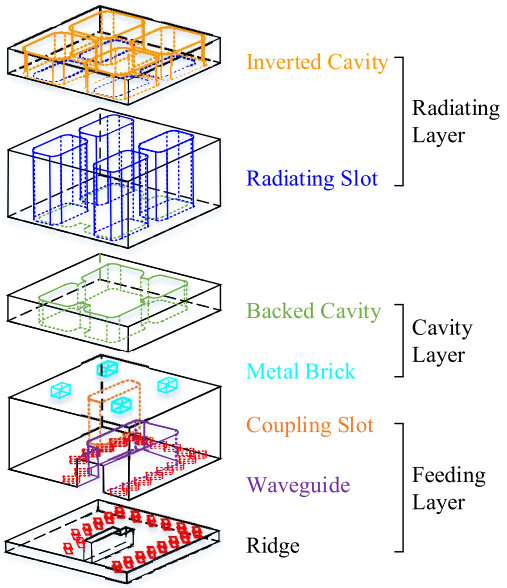

FIGURE 8. Configuration of the radiator with a 2 × 2 subarray radiator. The parameters of the radiator with a 2 × 2 subarray radiator are provided in Table 2.

TABLE 2. The parameters of the radiator with 2 × 2 subarray radiator.

Parameter	Value (mm)	Parameter	Value (mm)	Parameter	Value (mm)
L_{ic}	2.33	W_{ic}	2.90	H_{ic}	1.22
L_{rs}	1.44	W_{rs}	2.58	H_{rs}	3.12
L_{bc}	4.23	W_{bc}	5.52	H_{bc}	1.15
L_{mb}	0.45	W_{mb}	0.73	H_{mb}	0.37
L_{cs}	0.84	W_{cs}	2.85	H_{cs}	2.00
L_{w}	2.44	W_{w}	5.38	H_{w}	1.30
L_{r}	0.42	W_{r}	2.92	H_{r}	0.95
L_{bc1}	0.74	W_{bc1}	0.52	W_{w1}	0.40
L_{w1}	1.50	w_{r1}	0.93	H_{r1}	0.70

the unwanted higher mode of the original rectangular backed cavities, while the four rectangular metallic bricks are placed just directly beneath each radiation slot which can improve the bandwidth performance of the radiator [18]–[20].

The radiating layer is placed on the top of the whole 2×2 subarray radiator, which is constituted by radiating slots and inverted cavities, as shown in Fig. 8. The inverted cavities are added to suppress the mutual coupling between adjacent slots of the radiator Fig. 9 shows the simulated reflection coefficient and the radiation pattern of the designed subarray radiator. It is seen that the simulated bandwidth with a return loss (RL) larger than 10 dB is achieved from 67.8 GHz to almost 87 GHz, which means that the distribution network supplies enough bandwidth. In addition, the far-field radiation patterns at 79 GHz are simulated as shown in Fig. 10 to demonstrate the radiation characteristics of the designed sub-array radiator, and the simulated gain of the radiator is higher than 15 dBi.

B. THE WAVEGUIDE SLOT ARRAY ANTENNA DESIGN

Finally, the designed 2 × 2 subarray radiators and the T-junction power divider achieved by the integrated-EBG rectangular gap ridge waveguide are combined together to

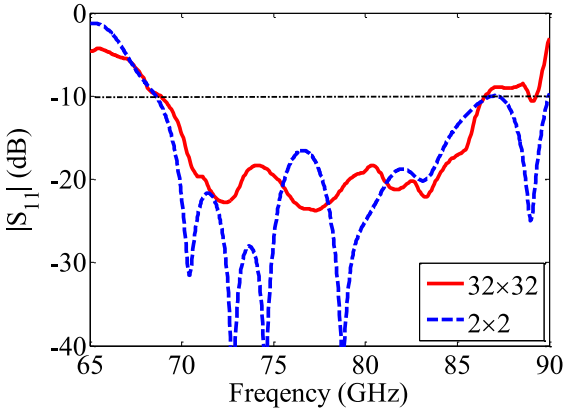

FIGURE 9. Simulated reflection coefficient of the radiator with 2 × 2 element subarray and the E-band box-horn antenna with 32 × 32 elements.

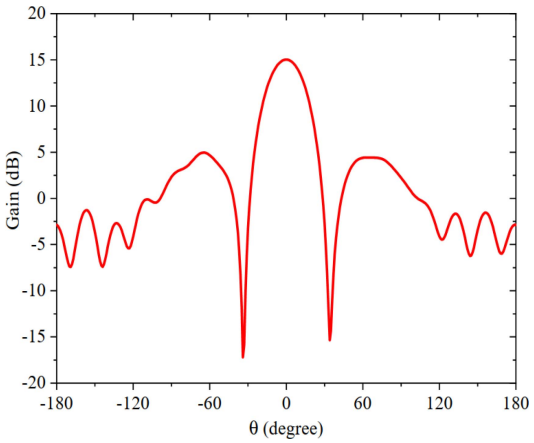

FIGURE 10. Simulated radiation pattern at 79 GHz of the radiator with 2 × 2 element subarray.

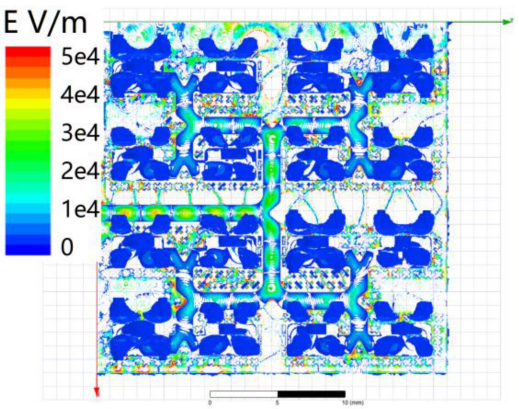

FIGURE 11. Simulated E-field on the designed E-band box-horn antenna with 32 × 32 elements and distribution networks at 79 GHz.

realize the whole waveguide 32x32 slot array antenna as shown in Fig. 1. The simulated reflection coefficient of the proposed array is below −10 dB from 70.8 to 87.6 GHz as shown in Fig. 9.

Fig. 11 shows the electric field distributions on the designed E-band box-horn antenna with 32×32 elements and

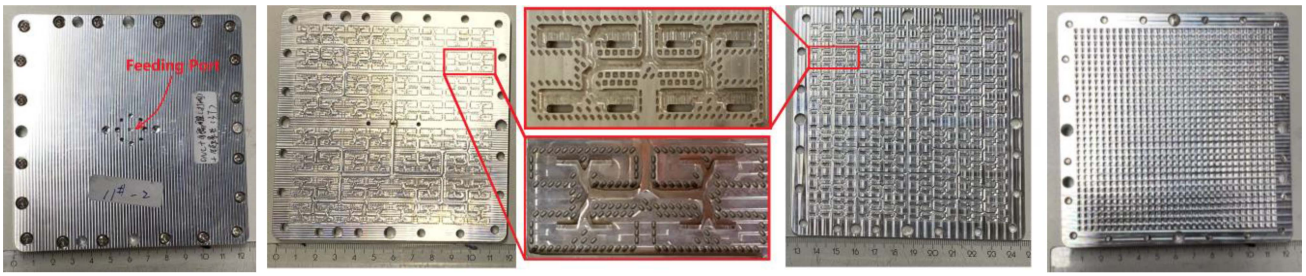

FIGURE 12. Photograph of the fabricated E-band box-horn antenna with 32 × 32 elements. (a) Bottom lay with feeding port. The ridge layer (b) and the waveguide layer (c) of the power divider realized by the gapped ridge waveguide with cross-shaped groove EBG structure. (d) Top view of the radiating layer.

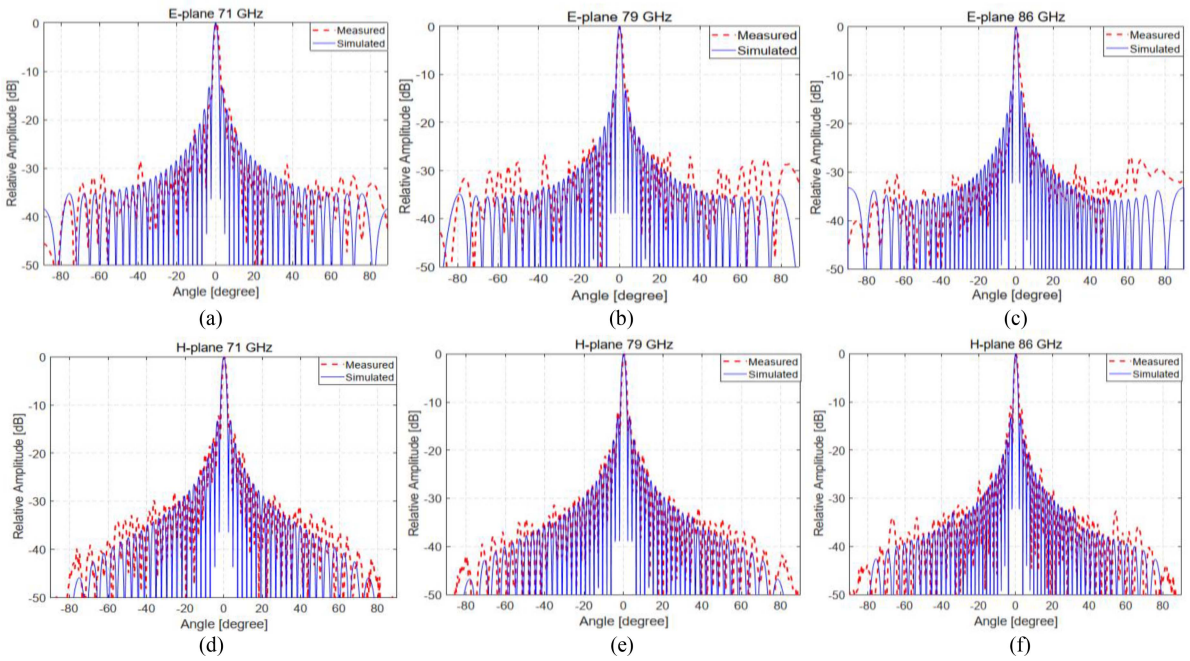

FIGURE 13. Simulated and measured radiation patterns of the designed E-band box-horn antenna with 32 × 32 elements.(a) E-plane at 71GHz. (b) E-plane at 79GHz. (c) E-plane at 86GHz. (d) H-plane at 71GHz. (e) H-plane at 79GHz. (f) H-plane at 86GHz.

distribution networks at 79 GHz, and comparatively uniform radiations are obtained at each subarray radiators. Fig. 13 shows the simulated normalized far-field radiation patterns of the antenna at 71, 79 and 86 GHz in E- and H-planes. It can be seen that a good radiation beam is generated by the designed waveguide slot array antenna, and the simulated main lobe points to the broadside direction with peak gain of 39.3 dBi at 79 GHz. Here, commercial ANSYS HFSS software is used and periodic boundary condition is set for simulation time saving, thanks to array's geometry symmetry in both longitudinal and lateral direction.

IV. MEASUREMENTS AND DISCUSSION

To verify the proposed methodology of designing the waveguide 32 × 32 slot array antenna realized by the integrated-EBG ridge waveguide, a prototype is designed and measured. All the studied microwave circuits are fabricated and assembled together to form the entire array antenna by screws. The whole slot antenna is separated into three metallic plates in order to be fabricated easily, and as shown in Fig. 12. The radiating layer including inverted cavities and radiating slots shown in Fig. 8 is fabricated together with the backed cavities of the cavity layer as the first plate of the antenna. Then, the metal brick of the cavity layer and the coupling slots together with the waveguide layer of the feeding layer are mounded as the second plate. Finally, the whole ridge layer of the whole distribution power divider network is manufactured as the third plate.

All the plates are processed by the Fanuc α-D14MiA CNC machine with manufacture tolerance of 2.5μm, and each plate is milled and drilled in both the front and back sides. In addition, during the whole fabrication process, the location of the upper and down metallic plate is precisely positioned, and several location holes are drilled on each metallic plate for stringing together and fastening with alignment pins. Fig. 14 shows the measured reflection coefficient of the

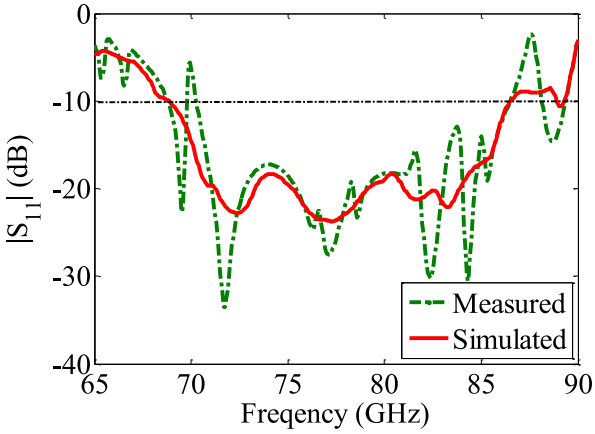

FIGURE 14. Measured and simulated reflection coefficient of the designed E-band box-horn antenna with 32 × 32 element.

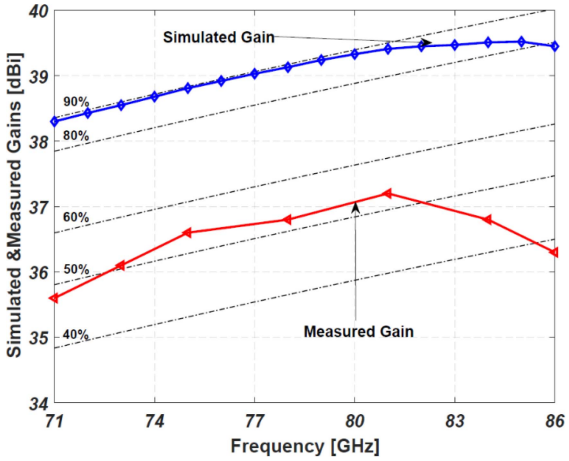

FIGURE 15. Measured and simulated gain of the designed E-band box-horn antenna with 32 × 32 element.

whole waveguide 32 × 32 slot array antenna with good performance below −10 dB from 70.6 to 86.8 GHz. It should be pointed out that the measured response with the prescribed frequency responses is very acceptable, although a discrepancy is observed and there is a dip in the reflection coefficients at around 70 GHz with the return loss nearly up to 7 dB. It means that the simple assembly process with metallic screws will provide sufficient conjunction, and the leakage loss because of the gap is weak enough and it can be ignored.

Then, the radiation patterns of antenna are measured to further validate the performance of the designed antenna based on the integrated-EBG gap ridge waveguide. The near-field measurement system is adopted by testing the antenna surface scanned by the vector network analyzer connected with the frequency multiplier, and the far-field radiation patterns are then calculated by transforming the scanned near-field measurement results. The measured normalized results at 71, 79 and 86 GHz as shown in Fig. 13. The simulated and measured prototype's gains as shown in Fig. 15. It can be seen the measured results is almost 37 dBi at 79 GHz with radiation efficiency about 52%, which is a reasonable agreement between the measured and prediction results.

V. CONCLUSION

A thin planer mmWave waveguide array antenna with high-efficiency and low-cost manufacturing properties has been proposed in this article based on integrated cross rectangle-hollow EBG structures. The dispersion diagram of the EBG structure is investigated, which shows the EBG structure supports no mode from 62 GHz to 89 GHz and prevents the leakage in gaped ridge waveguide structures with an unconnected gap in between the two metallic plates. Hence, the structure can be manufactured just by using of low-cost assembly methods. The antenna has been fabricated and its radiation characteristics have been demonstrated, while the measured gain is 37dBi. Both simulated and measured results have shown that the proposed integrated EBG ridge waveguide is a promising candidate for mmWave antennas.

REFERENCES

[1] *Allocation and Service Rules for the 71–76 GHz, 81–86 GHz, and 92–95 GHz Bands*, FCC, Washington, DC, USA, 2003.
[2] D. Lockie and D. Peck, "High-data-rate millimeter-wave radios, *IEEE Microw. Mag.*, vol. 10, no. 5, pp. 75–83, Aug. 2009.
[3] X. Li, J. Xiao, and J. Yu, "Long-distance wireless mm-Wave signal delivery at *w*−band," *J. Lightw. Technol.*, vol. 34, no. 2, pp. 661–668, Jan. 15, 2016.
[4] F. Greco, G. Amendola, L. Boccia, and E. Arnieri, "A dual band hat feed for reflector antennas in Q-V band," in *Proc. 10th Eur. Conf. Antennas Propag. (EuCAP)*, Apr. 2016, pp. 1–4.
[5] J. Hirokawa and M. Ando, "Efficiency of 76-GHz post-wall waveguide-fed parallel-plate slot arrays," *IEEE Trans. Antennas Propag.*, vol. 48,no. 11, pp. 1742–1745, Nov. 2000.
[6] H. Wang, D. Fang, B. Zhang, and W. Che, "Dielectric loaded substrate integrated waveguide (SIW) H-plane horn antennas," *IEEE Trans Antennas Propag.*, vol. 58, no. 3, pp. 640–647, Mar. 2010.
[7] B. A. Munk, *Frequency Selective Surfaces Theory and Design*. New York, NY, USA: Wiley, 2000.
[8] M. Ohira, A. Miura, and M. Ueba, "60-GHz wideband substrate-integrated waveguide slot array using closely spaced elements for planar multisector antenna," *IEEE Trans. Antennas Propag.*, vol. 58, no. 3, pp. 993–998, Mar. 2010.
[9] Y. Zhang, Z. N. Chen, X. Qing, and W. Hong, "Wideband millimeter-wave substrate integrated waveguide slotted narrow-wall fed cavity antennas," *IEEE Trans. Antennas Propag.*, vol. 59, no. 5, pp. 1488–1496, May 2011.
[10] O. Kramer, T. Djerafi, and K. Wu, "Very small footprint 60 GHz stacked YAGI antenna array," *IEEE Trans. Antennas Propag.*, vol. 59, no. 9, pp. 3204–3210, Sep. 2011.
[11] W. M. Abdel-Wahab and S. Safavi-Naeini, "Wide-bandwidth 60-GHz aperture-coupled microstrip patch antennas (MPAS) fed by substrate integrated waveguide (SIW)," *IEEE Antennas Wireless Propag. Lett.*, vol. 10, pp. 1003–1005, 2011.
[12] Y. J. Cheng, W. Hong, and K. Wu, "94 GHz substrate integrated monopulse antenna array," *IEEE Trans. Antennas Propag.*, vol. 60, no. 1, pp. 121–129, Jan. 2012.
[13] L. Wang, Y. J. Cheng, D. Ma, and C. X. Weng, "Wideband and dual-band high-gain substrate integrated antenna array for E-band multi-gigahertz capacity wireless communication systems," *IEEE Trans. Antennas Propag.*, vol. 62, no. 9, pp. 4602–4611, Sep. 2014.
[14] D. Deslandes and K. Wu, "Integrated microstrip and rectangular waveguide in planar form," *IEEE Microw. Wireless Compon. Lett.*, vol. 11, no. 2, pp. 68–70, Feb. 2001.
[15] N. Ghassemi and K.-M. Wu, "High-efficient patch antenna array for e-band gigabyte point-to-point wireless services," *IEEE Antennas Wireless Propagat. Lett.*, vol. 11, pp. 1261–1264, 2012.

[16] Y. Li and K. Luk, "Low-cost high-gain and broadband substrate-integrated-waveguide-fed patch antenna array for 60-GHz band," *IEEE Trans. Antennas Propag.*, vol. 62, no. 11, pp. 5531–5538, Aug. 2014.
[17] Y. Li and K.-M. Luk, "60-GHz substrate integrated waveguide fed cavity-backed aperture-coupled microstrip patch antenna arrays," *IEEE Trans. Antennas Propag.*, vol. 63, no. 3, pp. 1075–1085, Mar. 2015.
[18] Y. Miura, J. Hirokawa, M. Ando, Y. Shibuya, and G. Yoshida, "Double-layer full-corporate-feed hollow-waveguide slot array antenna in the 60-GHz band," *IEEE Trans. Antennas Propag.*, vol. 59, no. 8, pp. 2844–2851, Aug. 2011.
[19] D. Kim, J. Hirokawa, M. Ando, J. Takeuchi, and A. Hirata, "64 × 64-element and 32 × 32-element slot array antennas using double-layer hollow-waveguide corporate-feed in the 120 GHz band," *IEEE Trans. Antennas Propag.*, vol. 62, no. 3, pp. 1507–1512, Mar. 2014.
[20] P. Y. Liu, J. Liu, W. D. Hu, and X. M. Chen, "Hollow waveguide 32 × 32-slot array antenna covering 71-86 GHz band by the technology of a polyetherimide fabrication," *IEEE Antennas Wireless Propag. Lett.*, vol. 17, no. 9, pp. 1635–1638, Sep. 2018.
[21] E. Levine, G. Malamud, S. Shtrikman, and D. Treves, "A study of microstrip array antennas with the feed network," *IEEE Trans. Antennas Propag.*, vol. 37, no. 4, pp. 426–434, Apr. 1989.
[22] J. Wu, Y. J. Cheng, and Y. Fan, "A wideband high-gain high-efficiency hybrid integrated plate array antenna for *v*-band inter-satellite links," *IEEE Trans. Antennas Propag.*, vol. 63, no. 4, pp. 1225–1233, Apr. 2015.
[23] P.-S. Kildal, "Artificially soft and hard surfaces in electromagnetics," *IEEE Trans. Antennas Propag.*, vol. 38, no. 10, pp. 1537–1544, Oct. 1990.
[24] H. Raza, J. Yang, P. Kildal, and E. A. Als, "Microstrip-ridge gap waveguide-study of losses, bends, and transition to WR-15," *IEEE Trans. Microw. Theory Techn.*, vol. 62, no. 9, pp. 1943–1952, Jun. 2014.
[25] A. Vosoogh and P. Kildal, "Corporate-fed planar 60-GHz slot array made of three unconnected metal layers using AMC pin surface for the gap waveguide," *IEEE Antennas Wireless Propagat. Lett.*, vol. 15, pp. 1935–1938, 2016.
[26] A. Vosoogh, P. Kildal, and V. Vassilev, "Wideband and high-gain corporate-fed gap waveguide slot array antenna with ETSI class II radiation pattern in V-band," *IEEE Trans. Antennas Propag.*, vol. 65, no. 4, pp. 1823–1831, Apr. 2017.
[27] J. Liu, A. Vosoogh, A. U. Zaman, and J. Yang, "Design and fabrication of a high-gain 60-GHz cavity-backed slot antenna array fed by inverted microstrip gap waveguide," *IEEE Trans. Antennas Propag.*, vol. 65, no. 4, pp. 2117–2122, Apr. 2017.
[28] A. Farahbakhsh, D. Zarifi, and A. U. Zaman, "60-GHz groove gap waveguide based wideband H-plane power dividers and transitions: For use in high-gain slot array antenna," *IEEE Trans. Microw. Theory Technol.*, vol. 65, no. 11, pp. 4111–4121, Nov. 2017.
[29] J. Liu, A. Vosoogh, A. U. Zaman, and J. Yang, "A slot array antenna with single-layered corporate-feed based on ridge gap waveguide in the 60 GHz band," *IEEE Trans. Antennas Propag.*, vol. 67, no. 3, pp. 1650–1658, Mar. 2019.

ZHONGXIA SIMON HE (Senior Member, IEEE) received the M.Sc. degree from the Beijing Institute of Technology, Beijing, China, in 2008, and the Ph.D. degree from the Chalmers University of Technology, Göteborg, Sweden, in 2014, where he is currently an Assistant Professor with the Microwave Electronics Laboratory, Department of Microtechnology and Nanoscience (MC2). His current research interests include high data rate wireless communication, modulation and demodulation, mixed-signal integrated circuit design, radar, and packaging.

CHENG JIN (Senior Member, IEEE) received the B.Eng. degree in electronic engineering from the University of Electronic Science and Technology of China, Chengdu, China, in 2007, and the Ph.D. degree in communication engineering from Nanyang Technological University, Singapore, in 2012. From 2011 to 2013, he was with the Institute of Microelectronics, Agency for Science, Technology and Research, Singapore. Since January 2014, he has been as an Associate Professor with the School of Information and Electronics, Beijing Institute of Technology, Beijing, China. He has published and presented over 80 technical articles in journals/conferences. His current research interests include the design of microwave and millimeter-wave antennas, frequency selective surfaces and circuits, and microwave radar techniques.

SINING AN received the B.S. and M.Sc. degrees in communication and electronics engineering from the Beijing Institute of Technology, Beijing, China, in 2013 and 2016, respectively. She is currently pursuing the Ph.D. degree with the Microwave Electronics Laboratory, Department of Microtechnology and Nanoscience, Chalmers University of Technology. Her research interests include high data rate communication, modulation and demodulation, and high-resolution radar.

LINGWEN KONG was born in NeiMenggu, China, in 1997. She received the B.S. degree from the Communication University of China, Beijing, China, in 2019. She is currently pursuing the M.S. degree in electronic science and technology with the Beijing Institute of Technology, Beijing.

JINLIN LIU (Member, IEEE) received the B.Sc. degree in communications engineering from the University of Electronic Science and Technology of China, Chengdu, China, in 2005, the Vordiploma degree from the Munich University of Technology, Munich, Germany, in 2011, and the Swedish Licentiate degree and the Ph.D. degree from the Chalmers University of Technology, Gothenburg, Sweden, in 2016 and 2019, respectively.

From 2005 to 2007, he was with Intel, Chengdu branch, as a Test Engineer. From 2013 to 2014, he was with Eurodesign GmbH, Munich, as a PCB Test Engineer. His current research interests include fundamental electromagnetic theory, millimeter-wave planar antennas in general, gap waveguide technology, and frequency-selective surfaces. He received the Best Student Paper Award First Place at the 2017 International Symposium on Antennas and Propagation. He serves on the Reviewer Board for several journals, including the IEEE TRANSACTIONS ON ANTENNAS AND PROPAGATION, the IEEE TRANSACTIONS ON MICROWAVE THEORY AND TECHNIQUES, the IEEE TRANSACTIONS ON COMPONENTS, PACKAGING, AND MANUFACTURING, the IEEE ANTENNAS AND WIRELESS PROPAGATION LETTERS, the IEEE MICROWAVE AND WIRELESS COMPONENTS LETTERS, and the *Journal of Electromagnetic Waves and Applications*.